COMMUNICATIONS IN COMPUTATIONAL PHYSICS
Vol. 4, No. 1, pp. 1-25

Commun. Comput. Phys.
July 2008

Colocated Finite Volume Schemes for Fluid Flows

S. Faure[1], J. Laminie[1,2] and R. Temam[1,3,*]

[1] *Laboratoire de Mathématiques, Université Paris-Sud, Bâtiment 425, 91405 Orsay, France.*
[2] *GRIMAAG Guadeloupe, Université des Antilles et de la Guyane, Campus de Fouillole, BP 592, 97157 Pointe à Pitre Cedex, France.*
[3] *Institute for Scientific Computing and Applied Mathematics, Indiana University, Bloomington, IN 47405, USA.*

Received 11 September 2007; Accepted (in revised version) 10 February 2008

Communicated by Jie Shen

Available online 27 February 2008

Abstract. Our aim in this article is to improve the understanding of the colocated finite volume schemes for the incompressible Navier-Stokes equations. When all the variables are colocated, that means here when the velocities and the pressure are computed at the same place (at the centers of the control volumes), these unknowns must be properly coupled. Consequently, the choice of the time discretization and the method used to interpolate the fluxes at the edges of the control volumes are essentials. In the first and second parts of this article, two different time discretization schemes are considered with a colocated space discretization and we explain how the unknowns can be correctly coupled. Numerical simulations are presented in the last part of the article. This paper is not a comparison between staggered grid schemes and colocated schemes (for this, see, e.g., [15, 22]). We plan, in the future, to use a colocated space discretization and the multilevel method of [4] initially applied to the two dimensional Burgers problem, in order to solve the incompressible Navier-Stokes equations. One advantage of colocated schemes is that all variables share the same location, hence, the possibility to use hierarchical space discretizations more easily when multilevel methods are used. For this reason, we think that it is important to study this family of schemes.

AMS subject classifications: 76M12, 76D05, 68U120, 74S10, 74H15
Key words: Finite volumes, colocated scheme.

1 Introduction

We consider the Navier-Stokes equations in their velocity-pressure formulation and the continuity equation written for an incompressible viscous fluid; Ω is an open bounded

*Corresponding author. *Email addresses:* sylvain.faure@math.u-psud.fr (S. Faure), jacques.laminie@univ-ag.fr (J. Laminie), temam@indiana.edu (R. Temam)

domain in $\mathbb{R}^2$, for our simulations we use a rectangular domain $\Omega = (0,L_1)\times(0,L_2)$.
For given volume forces $\mathbf{f} = (f_u, f_v)$, we look for the velocity vector $\mathbf{u}$ and the pressure p such that:

$$\frac{\partial \mathbf{u}}{\partial t} - \nu \triangle \mathbf{u} + (\mathbf{u}\cdot\nabla)\mathbf{u} + \nabla p = \mathbf{f} \quad \text{in } \Omega\times[0,T], \tag{1.1}$$

$$div\, \mathbf{u} = 0, \tag{1.2}$$

where $\nu > 0$ is the kinematic viscosity and, in space dimension two, $\mathbf{u} = \big(u(x,y,t), v(x,y,t)\big)$, $t \geq 0$.

On the boundary $\partial\Omega$ of Ω, we impose a Dirichlet no-slip boundary condition:

$$\mathbf{u}\Big|_{\partial\Omega} = \mathbf{g}, \tag{1.3}$$

where $\mathbf{g} = (g_u, g_v)$ is a given function defined on $\partial\Omega$.

Traditionnally, the staggered variable arrangement was prefered to a colocated variable arrangement. Indeed, the colocated arrangements have long been considered as impracticable since these colocated schemes were known to generate a decoupling between the velocities and the pressure. This difficulty was subsequently resolved using appropriate interpolations of the fluxes (see below, e.g., (2.15)). Based on this idea, the first successful colocated finite volume schemes were introduced in 1981 by Hsu [9], Prakash [16] and Rhie [18]. A further advantage of colocated schemes is that they can be easily used for complex geometries [25]. Moreover, multilevel techniques, which result in a significant reduction of computing time on fine grids, are also much easier to apply to the colocated arrangement; this is an essential point regarding our objective to implement multilevel methods for the Navier-Stokes equations [4]. See [15, 22] for a detailed comparison between staggered and colocated schemes. We intend in a subsequent work [5] to combine the multilevel method presented in [4] with the colocated schemes described here. For theoretical aspects of the finite volume methods, see [2].

The purpose of the present article is to describe two colocated schemes associated with different time discretizations. For each scheme, we will study if there exists a decoupling between the velocities and the pressure. Then, we will comment on the numerical results obtained in the case of a driven cavity. Note that the emphasis here is on the development of the method only and therefore the driven cavity flow is not studied with too challenging values of the Reynolds number.

In the following, the domain Ω is discretized by rectangular finite volumes of same dimensions $\Delta x \Delta y$ with $M\Delta x = L_1$ and $N\Delta y = L_2$ (M, N are given integers). Hence, we have MN volumes which are defined (see Fig. 1) by:

$$\Big(K_{ij} = [x_{i-\frac{1}{2}}, x_{i+\frac{1}{2}}]\times[y_{j-\frac{1}{2}}, y_{j+\frac{1}{2}}]\Big)_{i=1,\cdots,M,\, j=1,\cdots,N},$$

where

$$x_{i+\frac{1}{2}} = i\Delta x \text{ for } i = 0,\cdots,M,$$
$$y_{j+\frac{1}{2}} = j\Delta y \text{ for } j = 0,\cdots,N.$$

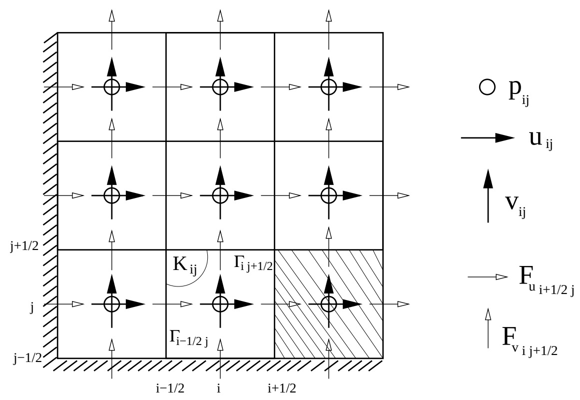

Figure 1: Colocated mesh.

The edges of the control volumes are defined by:

$$\Gamma_{i+\frac{1}{2}j} = \Big\{ (x,y)\,;\, x = x_{i+\frac{1}{2}}, y \in [y_{j-\frac{1}{2}}, y_{j+\frac{1}{2}}] \Big\} \text{ for } i=0,\cdots,M,$$
$$\Gamma_{ij+\frac{1}{2}} = \Big\{ (x,y)\,;\, x \in [x_{i-\frac{1}{2}}, x_{i+\frac{1}{2}}], y = y_{j+\frac{1}{2}}, \Big\} \text{ for } j=0,\cdots,N.$$

When a colocated method is used, all the unknowns, i.e. the velocities and the pressure, are defined at the center of the cells. Hence, for $i=1,\cdots,M$ and $j=1,\cdots,N$, the unknowns are meant to be approximations of the cell averages:

$$\mathbf{u}_{ij}(t) \simeq \frac{1}{\Delta x \Delta y} \int_{x_{i-\frac{1}{2}}}^{x_{i+\frac{1}{2}}} \int_{y_{j-\frac{1}{2}}}^{y_{j+\frac{1}{2}}} \mathbf{u}(x,y,t)\,dxdy \quad \text{for the velocity,} \tag{1.4}$$
$$p_{ij}(t) \simeq \frac{1}{\Delta x \Delta y} \int_{x_{i-\frac{1}{2}}}^{x_{i+\frac{1}{2}}} \int_{y_{j-\frac{1}{2}}}^{y_{j+\frac{1}{2}}} p(x,y,t)\,dxdy \quad \text{for the pressure.} \tag{1.5}$$

Remark 1.1. Notice that, in order to simplify the notations for the boundary conditions, we also introduce fictitious control volumes:

$$\Big(K_{0j} = [x_{-\frac{1}{2}}, x_{\frac{1}{2}}] \times [y_{j-\frac{1}{2}}, y_{j+\frac{1}{2}}] \text{ and } K_{M+1j} = [x_{M+\frac{1}{2}}, x_{M+\frac{3}{2}}] \times [y_{j-\frac{1}{2}}, y_{j+\frac{1}{2}}] \Big)_{j=1,\cdots,N}$$
$$\Big(K_{i0} = [x_{i-\frac{1}{2}}, x_{i+\frac{1}{2}}] \times [y_{-\frac{1}{2}}, y_{\frac{1}{2}}] \text{ and } K_{iN+1} = [x_{i-\frac{1}{2}}, x_{i+\frac{1}{2}}] \times [y_{N+\frac{1}{2}}, y_{N+\frac{3}{2}}] \Big)_{i=1,\cdots,M}$$

where $x_{-\frac{1}{2}} = -\Delta x$, $x_{M+\frac{3}{2}} = L_1 + \Delta x$, $y_{-\frac{1}{2}} = -\Delta y$ and $y_{N+\frac{3}{2}} = L_2 + \Delta y$. Consequently, for the Dirichlet boundary condition on the velocity, we will write

$$\mathbf{u}_{0j} = 2\mathbf{g}_{\frac{1}{2}j} - \mathbf{u}_{1j}$$

(see, e.g., (2.6)), and, for the Neumann boundary condition on the pressure, we will write $p_{0j} = p_{1j}$ (see, e.g.,(2.7)).

Furthermore, we also define the velocity fluxes which occur in the schemes, in the nonlinear terms for example:

$$F_{u\,i+\frac{1}{2}j}(t) \simeq \frac{1}{\Delta y}\int_{y_{j-\frac{1}{2}}}^{y_{j+\frac{1}{2}}} u(x_{i+\frac{1}{2}},y,t)\,dy \;\text{ for the horizontal fluxes,} \quad i=0,\cdots,M, \tag{1.6}$$

$$F_{v\,ij+\frac{1}{2}}(t) \simeq \frac{1}{\Delta x}\int_{x_{i-\frac{1}{2}}}^{x_{i+\frac{1}{2}}} v(x,y_{j+\frac{1}{2}},t)\,dx \;\text{ for the vertical fluxes,} \quad j=0,\cdots,N. \tag{1.7}$$

However, as we shall see, the velocity fluxes are not considered as independant unknowns: they will be computed either directly or by interpolation from the above cell centered unknowns (1.4), (1.5).

Finally, concerning the time discretization of the problem (1.1)-(1.3), let $T>0$ be fixed, and let the time step be $\Delta t = T/N_t$ where N_t is an integer. For $k=0,\cdots,N_t$, we define $\mathbf{u}^k$ as the approximate value of $\mathbf{u}$ at the time $t_k = k\Delta t$. In the following we will use a time finite difference scheme to approximate the time derivative. Hence, we will not use a space-time finite volume discretization but a space finite volume discretization with a time finite difference scheme. An advantage of this choice is that time implicit discretizations for the diffusive terms can be considered.

In the next section, we describe the colocated scheme associated with the projection method of Van Kan [21]. In the third section, we present the scheme associated with the new splitting method of Guermond and Shen [7]. Then, in the last section we present the numerical results obtained with both schemes and give some comments.

2 A colocated finite volume scheme with a projection method for the time discretization

2.1 Time discretization

The concept of projection methods was introduced by [1, 20] in the late 60s, extending to the Navier-Stokes equations the concepts of fractional step methods [12, 23, 24]. Then, several projection methods have been elaborated, see [8, 10, 13, 19] producing schemes of order two in time in general. In this section, we consider for simplicity the projection method of Van Kan [21]; we will study in a future work the improvements resulting from more recent projection methods.

We start from a Crank-Nicholson scheme for the linear part and an Adams-Bashforth scheme for the nonlinear part, that is:

$$\begin{cases} \dfrac{\mathbf{u}^{n+1}-\mathbf{u}^n}{\Delta t} - \nu\triangle\Big(\dfrac{\mathbf{u}^{n+1}+\mathbf{u}^n}{2}\Big) + \mathcal{B}\left(\mathbf{u}^n,\mathbf{u}^{n-1}\right) + \nabla\Big(\dfrac{p^{n+1}+p^n}{2}\Big) = \dfrac{\mathbf{f}^{n+1}+\mathbf{f}^n}{2}, \\ \mathbf{u}^{n+1}\Big|_{\partial\Omega} = \mathbf{g}^{n+1}, \\ div\,\mathbf{u}^{n+1} = 0, \end{cases} \tag{2.1}$$

where $\mathcal{B}\left(\mathbf{u}^n,\mathbf{u}^{n-1}\right)=\frac{3}{2}(\mathbf{u}^n.\nabla)\mathbf{u}^n-\frac{1}{2}(\mathbf{u}^{n-1}.\nabla)\mathbf{u}^{n-1}$.

Combining this with the projection scheme we obtain:

$$\left\{\begin{array}{l}\dfrac{\mathbf{u}^{n+\frac{1}{2}}-\mathbf{u}^n}{\Delta t}-\nu\triangle\Big(\dfrac{\mathbf{u}^{n+\frac{1}{2}}+\mathbf{u}^n}{2}\Big)+\mathcal{B}\left(\mathbf{u}^n,\mathbf{u}^{n-1}\right)+\nabla p^n=\dfrac{\mathbf{f}^{n+1}+\mathbf{f}^n}{2},\\ \mathbf{u}^{n+\frac{1}{2}}\Big|_{\partial\Omega}=\mathbf{g}^{n+1},\end{array}\right. \tag{2.2}$$

$$\left\{\begin{array}{l}\dfrac{\mathbf{u}^{n+1}-\mathbf{u}^{n+\frac{1}{2}}}{\Delta t}=-\dfrac{1}{2}\nabla\delta p^{n+1}\text{ where }\delta p^{n+1}=p^{n+1}-p^n,\\ div\,\mathbf{u}^{n+1}=0,\\ \mathbf{u}^{n+1}\cdot\mathbf{n}\Big|_{\partial\Omega}=\mathbf{g}^{n+1}\cdot\mathbf{n}\Big|_{\partial\Omega};\end{array}\right. \tag{2.3}$$

$\mathbf{u}^{n+\frac{1}{2}}$ is called the intermediate velocity.

Moreover, from (2.2) and (2.3), we deduce the following Neuman problem used to compute the increment to the pressure:

$$\left\{\begin{array}{l}\triangle\delta p^{n+1}=\dfrac{2}{\Delta t}div\,\mathbf{u}^{n+\frac{1}{2}},\\ \dfrac{\partial\delta p^{n+1}}{\partial\mathbf{n}}=0.\end{array}\right. \tag{2.4}$$

The proposed algorithm starts by computing the intermediate velocities using (2.2). Then, in the second step, the projection step, we compute the pressure with (2.4). The new velocities are finally derived from (2.3). Consequently, the computations of the velocity and the pressure are decoupled. As the nonlinear terms are made explicit, at each time step, we only have to solve a set of Helmholtz-type equations for the velocity and a scalar Poisson equation with Neumann boundary condition for the pressure. Another advantage of this method is that the incompressibility condition is satisfied with the computer accuracy.

2.2 Finite volume discretization

Now, we describe the spatial discretization, that is the colocated finite volume implementation of the previous time discretization. As usual in a finite volume context, we integrate the equations on each control volume K_{ij} for $i=1,\cdots,M$, $j=1,\cdots,N$, and we find:

- For the time derivative term in (2.2):

$$\int_{K_{ij}}\frac{\mathbf{u}^{n+\frac{1}{2}}-\mathbf{u}^n}{\Delta t}dxdy\simeq\Delta x\Delta y\frac{\mathbf{u}_{ij}^{n+\frac{1}{2}}-\mathbf{u}_{ij}^n}{\Delta t}.$$

- For the Laplace operator used with the velocities in (2.2) and with the pressure variation in (2.4):

$$\int_{K_{ij}} \triangle \mathbf{u}\, dxdy = \int_{\partial K_{ij}} \frac{\partial \mathbf{u}}{\partial n} d\Gamma$$
$$\simeq \Delta y \frac{\mathbf{u}_{i+1j}-\mathbf{u}_{ij}}{\Delta x} + \Delta y \frac{\mathbf{u}_{i-1j}-\mathbf{u}_{ij}}{\Delta x} + \Delta x \frac{\mathbf{u}_{ij+1}-\mathbf{u}_{ij}}{\Delta y} + \Delta x \frac{\mathbf{u}_{ij-1}-\mathbf{u}_{ij}}{\Delta y},$$
$$\int_{K_{ij}} \triangle \delta p\, dxdy \simeq \Delta y \frac{\delta p_{i+1j}-\delta p_{ij}}{\Delta x} + \Delta y \frac{\delta p_{i-1j}-\delta p_{ij}}{\Delta x} + \Delta x \frac{\delta p_{ij+1}-\delta p_{ij}}{\Delta y} + \Delta x \frac{\delta p_{ij-1}-\delta p_{ij}}{\Delta y}.$$

- For the pressure gradient used in (2.2) and (2.3):

$$\int_{K_{ij}} \nabla p\, dxdy = \int_{\partial K_{ij}} \begin{pmatrix} pn_x \\ pn_y \end{pmatrix} d\Gamma \simeq \begin{pmatrix} \dfrac{\Delta y}{2}\left(p_{i+1j}-p_{i-1j}\right) \\ \dfrac{\Delta x}{2}\left(p_{ij+1}-p_{ij-1}\right) \end{pmatrix},$$

using a linear interpolation for the pressure at the edges.

- For the nonlinear term in (2.2):

$$\int_{K_{ij}} (\mathbf{u}\cdot\nabla)\mathbf{u}\, dxdy = \int_{K_{ij}} \begin{pmatrix} \partial_x(u^2)+\partial_y(vu) \\ \partial_x(uv)+\partial_y(v^2) \end{pmatrix} dxdy$$
$$= \int_{\partial K_{ij}} \begin{pmatrix} (u^2)n_x+(vu)n_y \\ (uv)n_x+(v^2)n_y \end{pmatrix} d\Gamma$$
$$\simeq \begin{pmatrix} \Delta y F_{u\,i+\frac{1}{2}j} \dfrac{u_{i+1j}+u_{ij}}{2} - \Delta y F_{u\,i-\frac{1}{2}j} \dfrac{u_{ij}+u_{i-1j}}{2} \\ \Delta y F_{u\,i+\frac{1}{2}j} \dfrac{v_{i+1j}+v_{ij}}{2} - \Delta y F_{u\,i-\frac{1}{2}j} \dfrac{v_{ij}+v_{i-1j}}{2} \end{pmatrix}$$
$$+ \begin{pmatrix} \Delta x F_{v\,ij+\frac{1}{2}} \dfrac{u_{ij+1}+u_{ij}}{2} - \Delta x F_{v\,ij-\frac{1}{2}} \dfrac{u_{ij}+u_{ij-1}}{2} \\ \Delta x F_{v\,ij+\frac{1}{2}} \dfrac{v_{ij+1}+v_{ij}}{2} - \Delta x F_{v\,ij-\frac{1}{2}} \dfrac{v_{ij}+v_{ij-1}}{2} \end{pmatrix},$$

using again a linear interpolation for the velocities at the edges.

- For the divergence term in (2.4):

$$\int_{K_{ij}} div\,\mathbf{u}\, dxdy = \int_{\partial K_{ij}} \mathbf{u}\cdot\mathbf{n}\, d\Gamma$$
$$\simeq \left[\Delta y\left(F_{u\,i+\frac{1}{2}j} - F_{u\,i-\frac{1}{2}j}\right) + \Delta x\left(F_{v\,ij+\frac{1}{2}} - F_{v\,ij-\frac{1}{2}}\right)\right].$$

Remark 2.1. In all the following of the paper when we will study two time discretizations, the nonlinear term will be written in an explicit form. However, it is also possible to modify the above space discretization in order to then use a semi-implicit form.

In the above equations, the boundary conditions are not taken into account. The Dirichlet boundary condition for the intermediate velocity $\mathbf{u}^{n+\frac{1}{2}}$ in (2.2) means that for $i=1,\cdots,M$ and $j=1,\cdots,N$, we have:

$$\mathbf{u}_{M+\frac{1}{2}j}^{n+\frac{1}{2}}=\mathbf{g}_{M+\frac{1}{2}j}^{n+1},\quad \mathbf{u}_{\frac{1}{2}j}^{n+\frac{1}{2}}=\mathbf{g}_{\frac{1}{2}j}^{n+1},\quad \mathbf{u}_{i\frac{1}{2}}^{n+\frac{1}{2}}=\mathbf{g}_{i\frac{1}{2}}^{n+1},\quad \mathbf{u}_{iN+\frac{1}{2}}^{n+\frac{1}{2}}=\mathbf{g}_{iN+\frac{1}{2}}^{n+1}, \tag{2.5}$$

which can be rewritten, due to the linear interpolation of the velocities at the edges, as follows:

$$\begin{aligned}
&\frac{\mathbf{u}_{M+1j}^{n+\frac{1}{2}}+\mathbf{u}_{Mj}^{n+\frac{1}{2}}}{2}=\mathbf{g}_{M+\frac{1}{2}j}^{n+1}, &&\frac{\mathbf{u}_{0j}^{n+\frac{1}{2}}+\mathbf{u}_{1j}^{n+\frac{1}{2}}}{2}=\mathbf{g}_{\frac{1}{2}j}^{n+1},\\
&\frac{\mathbf{u}_{i0}^{n+\frac{1}{2}}+\mathbf{u}_{i1}^{n+\frac{1}{2}}}{2}=\mathbf{g}_{i\frac{1}{2}}^{n+1}, &&\frac{\mathbf{u}_{iN+1}^{n+\frac{1}{2}}+\mathbf{u}_{iN}^{n+\frac{1}{2}}}{2}=\mathbf{g}_{iN+\frac{1}{2}}^{n+1},
\end{aligned} \tag{2.6}$$

where $\mathbf{g}_{M+\frac{1}{2}j}^{n+1}$, $\mathbf{g}_{\frac{1}{2}j}^{n+1}$, $\mathbf{g}_{iN+\frac{1}{2}}^{n+1}$ and $\mathbf{g}_{i\frac{1}{2}}^{n+1}$ are given by:

$$\begin{aligned}
&\mathbf{g}_{M+\frac{1}{2}j}^{n+1}=\frac{1}{\Delta y}\int_{y_{j-\frac{1}{2}}}^{y_{j+\frac{1}{2}}}\mathbf{g}(L_1,y,t_{n+1})\,dy, &&\mathbf{g}_{\frac{1}{2}j}^{n+1}=\frac{1}{\Delta y}\int_{y_{j-\frac{1}{2}}}^{y_{j+\frac{1}{2}}}\mathbf{g}(0,y,t_{n+1})\,dy,\\
&\mathbf{g}_{iN+\frac{1}{2}}^{n+1}=\frac{1}{\Delta x}\int_{x_{i-\frac{1}{2}}}^{x_{i+\frac{1}{2}}}\mathbf{g}(x,L_2,t_{n+1})\,dx, &&\mathbf{g}_{i\frac{1}{2}}^{n+1}=\frac{1}{\Delta x}\int_{x_{i-\frac{1}{2}}}^{x_{i+\frac{1}{2}}}\mathbf{g}(x,0,t_{n+1})\,dx.
\end{aligned}$$

It is well known that when we use finite volumes with Dirichlet boundary conditions, we consider the edges which determine the frontier of the domain as control volumes.

Moreover, the Neumann boundary condition for the pressure variation δp^{n+1} in (2.4) means that:

$$\delta p_{M+1j}^{n+1}=\delta p_{Mj}^{n+1},\quad \delta p_{0j}^{n+1}=\delta p_{1j}^{n+1},\quad \delta p_{i0}^{n+1}=\delta p_{i1}^{n+1},\quad \delta p_{iN+1}^{n+1}=\delta p_{iN}^{n+1}. \tag{2.7}$$

When Neumann boundary conditions are required in a finite volume context, we introduce virtual control volumes outside the domain.

Finally, the three steps of the method are the following:

Step 1. We compute the intermediate velocities $\mathbf{u}^{n+\frac{1}{2}}=\left(u^{n+\frac{1}{2}},v^{n+\frac{1}{2}}\right)$ from:

$$
\begin{aligned}
&\Delta x\Delta y\frac{\mathbf{u}_{ij}^{n+\frac{1}{2}}-\mathbf{u}_{ij}^{n}}{\Delta t}-\frac{\nu}{2}\left[\Delta y\frac{\mathbf{u}_{i+1j}^{n+\frac{1}{2}}-\mathbf{u}_{ij}^{n+\frac{1}{2}}}{\Delta x}+\Delta y\frac{\mathbf{u}_{i-1j}^{n+\frac{1}{2}}-\mathbf{u}_{ij}^{n+\frac{1}{2}}}{\Delta x}+\Delta x\frac{\mathbf{u}_{ij+1}^{n+\frac{1}{2}}-\mathbf{u}_{ij}^{n+\frac{1}{2}}}{\Delta y}\right.\\
&\left.+\Delta x\frac{\mathbf{u}_{ij-1}^{n+\frac{1}{2}}-\mathbf{u}_{ij}^{n+\frac{1}{2}}}{\Delta y}+\Delta y\frac{\mathbf{u}_{i+1j}^{n}-\mathbf{u}_{ij}^{n}}{\Delta x}+\Delta y\frac{\mathbf{u}_{i-1j}^{n}-\mathbf{u}_{ij}^{n}}{\Delta x}+\Delta x\frac{\mathbf{u}_{ij+1}^{n}-\mathbf{u}_{ij}^{n}}{\Delta y}+\Delta x\frac{\mathbf{u}_{ij-1}^{n}-\mathbf{u}_{ij}^{n}}{\Delta y}\right]\\
&+\frac{3}{2}\left[\Delta yF^{n}_{u\,i+\frac{1}{2}j}\frac{\mathbf{u}_{i+1j}^{n}+\mathbf{u}_{ij}^{n}}{2}-\Delta yF^{n}_{u\,i-\frac{1}{2}j}\frac{\mathbf{u}_{ij}^{n}+\mathbf{u}_{i-1j}^{n}}{2}+\Delta xF^{n}_{v\,ij+\frac{1}{2}}\frac{\mathbf{u}_{ij+1}^{n}+\mathbf{u}_{ij}^{n}}{2}\right.\\
&\left.-\Delta xF^{n}_{v\,ij-\frac{1}{2}}\frac{\mathbf{u}_{ij}^{n}+\mathbf{u}_{ij-1}^{n}}{2}\right]-\frac{1}{2}\left[\Delta yF^{n-1}_{u\,i+\frac{1}{2}j}\frac{\mathbf{u}_{i+1j}^{n-1}+\mathbf{u}_{ij}^{n-1}}{2}-\Delta yF^{n-1}_{u\,i-\frac{1}{2}j}\frac{\mathbf{u}_{ij}^{n-1}+\mathbf{u}_{i-1j}^{n-1}}{2}\right.\\
&\left.+\Delta xF^{n-1}_{v\,ij+\frac{1}{2}}\frac{\mathbf{u}_{ij+1}^{n-1}+\mathbf{u}_{ij}^{n-1}}{2}-\Delta xF^{n-1}_{v\,ij-\frac{1}{2}}\frac{\mathbf{u}_{ij}^{n-1}+\mathbf{u}_{ij-1}^{n-1}}{2}\right]+\begin{pmatrix}\frac{\Delta y}{2}\left(p_{i+1j}^{n}-p_{i-1j}^{n}\right)\\ \frac{\Delta x}{2}\left(p_{ij+1}^{n}-p_{ij-1}^{n}\right)\end{pmatrix}\\
=&\Delta x\Delta y\frac{\mathbf{f}_{ij}^{n+1}+\mathbf{f}_{ij}^{n}}{2},
\end{aligned}
\tag{2.8}
$$

using the boundary conditions (2.6) and (2.7).

Step 2. We compute the pressure variation δp^{n+1} from:

$$
\begin{aligned}
&\Delta y\frac{\delta p_{i+1j}^{n+1}-\delta p_{ij}^{n+1}}{\Delta x}+\Delta y\frac{\delta p_{i-1j}^{n+1}-\delta p_{ij}^{n+1}}{\Delta x}+\Delta x\frac{\delta p_{ij+1}^{n+1}-\delta p_{ij}^{n+1}}{\Delta y}+\Delta x\frac{\delta p_{ij-1}^{n+1}-\delta p_{ij}^{n+1}}{\Delta y}\\
=&\frac{2}{\Delta t}\left[\Delta y\left(F^{n+\frac{1}{2}}_{u\,i+\frac{1}{2}j}-F^{n+\frac{1}{2}}_{u\,i-\frac{1}{2}j}\right)+\Delta x\left(F^{n+\frac{1}{2}}_{v\,ij+\frac{1}{2}}-F^{n+\frac{1}{2}}_{v\,ij-\frac{1}{2}}\right)\right],
\end{aligned}
\tag{2.9}
$$

using the boundary conditions (2.7).

Step 3. We compute the new velocities $\mathbf{u}^{n+1}$ and the new fluxes F_u^{n+1} and F_v^{n+1} from:

$$
\Delta x\Delta y\frac{\mathbf{u}_{ij}^{n+1}-\mathbf{u}_{ij}^{n+\frac{1}{2}}}{\Delta t}=-\frac{1}{2}\begin{pmatrix}\frac{\Delta y}{2}\left(\delta p_{i+1j}^{n+1}-\delta p_{i-1j}^{n+1}\right)\\ \frac{\Delta x}{2}\left(\delta p_{ij+1}^{n+1}-\delta p_{ij-1}^{n+1}\right)\end{pmatrix},
\tag{2.10}
$$

$$
\frac{F^{n+1}_{u\,i+\frac{1}{2}j}-F^{n+\frac{1}{2}}_{u\,i+\frac{1}{2}j}}{\Delta t}=-\frac{1}{2}\frac{\delta p_{i+1j}^{n+1}-\delta p_{ij}^{n+1}}{\Delta x},
\tag{2.11}
$$

$$
\frac{F^{n+1}_{v\,ij+\frac{1}{2}}-F^{n+\frac{1}{2}}_{v\,ij+\frac{1}{2}}}{\Delta t}=-\frac{1}{2}\frac{\delta p_{ij+1}^{n+1}-\delta p_{ij}^{n+1}}{\Delta y},
\tag{2.12}
$$

using the boundary conditions (2.7).

In the above algorithm, at the first step we determine the intermediate velocities $\mathbf{u}^{n+\frac{1}{2}}$ at the center of the cells. However, for the second and third steps, we need to know the intermediate velocity fluxes $F_u^{n+\frac{1}{2}}$ and $F_v^{n+\frac{1}{2}}$, hence, these fluxes must be interpolated from the values of the intermediate velocities at the center of the cells. As this interpolation is crucial, we devote the next subsection to explain how we compute the fluxes.

2.3 Computation of the intermediate fluxes

The method of interpolation used to compute the intermediate fluxes is essential because it determines the coupling between the velocities and the pressure. The simplest method to compute the intermediate fluxes is the linear interpolation:

$$F^{n+\frac{1}{2}}_{u\,i+\frac{1}{2}j}=\frac{u^{n+\frac{1}{2}}_{i+1j}+u^{n+\frac{1}{2}}_{ij}}{2},\qquad F^{n+\frac{1}{2}}_{v\,ij+\frac{1}{2}}=\frac{v^{n+\frac{1}{2}}_{ij+1}+v^{n+\frac{1}{2}}_{ij}}{2}. \tag{2.13}$$

Unfortunately, this simple interpolation does not work when we reduce the viscosity ν because the pressure and the velocities are not sufficiently coupled. Let us emphasize this technical difficulty. First, if we consider that $\mathbf{u}^{n+\frac{1}{2}}$ is known, then, from (2.8), we obtain:

$$\begin{aligned}
u^{n+\frac{1}{2}}_{ij}=&\frac{1}{a}\Bigg[\frac{\Delta x\Delta y}{\Delta t}u^n_{ij}+\frac{\nu}{2}\Bigg[\frac{\Delta y}{\Delta x}u^{n+\frac{1}{2}}_{i+1j}+\frac{\Delta y}{\Delta x}u^{n+\frac{1}{2}}_{i-1j}+\frac{\Delta x}{\Delta y}u^{n+\frac{1}{2}}_{ij+1}+\frac{\Delta x}{\Delta y}u^{n+\frac{1}{2}}_{ij-1}\\
&+\Delta y\frac{u^n_{i+1j}-u^n_{ij}}{\Delta x}+\Delta y\frac{u^n_{i-1j}-u^n_{ij}}{\Delta x}+\Delta x\frac{u^n_{ij+1}-u^n_{ij}}{\Delta y}+\Delta x\frac{u^n_{ij-1}-u^n_{ij}}{\Delta y}\Bigg]\\
&-\frac{3}{2}\Bigg[\Delta yF^n_{u\,i+\frac{1}{2}j}\frac{u^n_{i+1j}+u^n_{ij}}{2}-\Delta yF^n_{u\,i-\frac{1}{2}j}\frac{u^n_{ij}+u^n_{i-1j}}{2}+\Delta xF^n_{v\,ij+\frac{1}{2}}\frac{u^n_{ij+1}+u^n_{ij}}{2}\\
&-\Delta xF^n_{v\,ij-\frac{1}{2}}\frac{u^n_{ij}+u^n_{ij-1}}{2}\Bigg]+\frac{1}{2}\Bigg[\Delta yF^{n-1}_{u\,i+\frac{1}{2}j}\frac{u^{n-1}_{i+1j}+u^{n-1}_{ij}}{2}-\Delta yF^{n-1}_{u\,i-\frac{1}{2}j}\frac{u^{n-1}_{ij}+u^{n-1}_{i-1j}}{2}\\
&+\Delta xF^{n-1}_{v\,ij+\frac{1}{2}}\frac{u^{n-1}_{ij+1}+u^{n-1}_{ij}}{2}-\Delta xF^{n-1}_{v\,ij-\frac{1}{2}}\frac{u^{n-1}_{ij}+u^{n-1}_{ij-1}}{2}\Bigg]+\Delta x\Delta y\frac{f^{n+1}_{u\,ij}+f^n_{u\,ij}}{2}\Bigg]\\
&-\frac{1}{a}\frac{\Delta y}{2}\left(p^n_{i+1j}-p^n_{i-1j}\right),
\end{aligned} \tag{2.14}$$

where

$$a=\Big(\frac{\Delta x\Delta y}{\Delta t}+\nu\frac{\Delta y}{\Delta x}+\nu\frac{\Delta x}{\Delta y}\Big).$$

Now, considering only the last term in the right hand side of the above equation, the contribution of the pressure in the horizontal fluxes computed with the linear interpolation (2.13) is:

$$-\frac{1}{a}\frac{\Delta y}{4}\left(p^n_{i+2j}+p^n_{i+1j}-p^n_{ij}-p^n_{i-1j}\right).$$

This implies that in the right hand side of (2.9), the pressure contribution to $\big(F^{n+\frac{1}{2}}_{u\,i+\frac{1}{2}j}-F^{n+\frac{1}{2}}_{u\,i-\frac{1}{2}j}\big)$ is $p^n_{i+2j}-2p^n_{ij}+p^n_{i-2j}$. This contribution shows that the pressure terms p^n_{i+1j} and p^n_{i-1j} do not play any role in the divergence of the intermediate velocity i.e. the velocity and the pressure are decoupled. Such an interpolation leads to incorrect numerical results when we increase the Reynolds number.

We have bypassed this difficulty using an approach proposed in [14,15,17]. We have modified the interpolation method for the intermediate fluxes. Let us now describe how we compute the horizontal fluxes (and the same method is used for the vertical fluxes):

$$\begin{aligned} F^{n+\frac{1}{2}}_{u\,i+\frac{1}{2}j} &= \frac{u^{n+\frac{1}{2}}_{i+1j}+u^{n+\frac{1}{2}}_{ij}}{2}+\frac{\Delta y}{4a}\Big(p^n_{i+2j}-2p^n_{i+1j}+p^n_{ij}\Big)-\frac{\Delta y}{4a}\Big(p^n_{i+1j}-2p^n_{ij}+p^n_{i-1j}\Big), \\ F^{n+\frac{1}{2}}_{v\,ij+\frac{1}{2}} &= \frac{v^{n+\frac{1}{2}}_{ij+1}+v^{n+\frac{1}{2}}_{ij}}{2}+\frac{\Delta x}{4a}\Big(p^n_{ij+2}-2p^n_{ij+1}+p^n_{ij}\Big)-\frac{\Delta x}{4a}\Big(p^n_{ij+1}-2p^n_{ij}+p^n_{ij-1}\Big). \end{aligned} \tag{2.15}$$

If we study the pressure contribution in the horizontal fluxes computed with this new interpolation (2.15) as for the linear interpolation (2.13), then we find:

$$-\frac{2\Delta y}{a}\Big(p^n_{i+1j}-p^n_{ij}\Big).$$

This implies that in the right hand side of (2.9), the pressure contribution in $\big(F^{n+\frac{1}{2}}_{u\,i+\frac{1}{2}j}-F^{n+\frac{1}{2}}_{u\,i-\frac{1}{2}j}\big)$ is $p^n_{i+1j}-2p^n_{ij}+p^n_{i-1j}$, i.e., the pressure and the velocity are well-coupled.

Remark 2.2. It is important to note that the above interpolation does not increase the cost of the simulation as we do not have to solve a new linear system in order to obtain the intermediate fluxes.

Remark 2.3. When we compare the linear interpolation (2.13) with the modified linear interpolation (2.15), we note that the added term corresponds to a third derivative of the pressure multiplied by Δx:

$$\begin{aligned} &\frac{\Delta y}{4a}\Big(p^n_{i+2j}-2p^n_{i+1j}+p^n_{ij}\Big)-\frac{\Delta y}{4a}\Big(p^n_{i+1j}-2p^n_{ij}+p^n_{i-1j}\Big) \\ &\simeq\left(\frac{1}{\Delta t}+\frac{\nu}{\Delta x^2}+\frac{\nu}{\Delta y^2}\right)^{-1}\left(\frac{\Delta x}{4}\left(\partial^3_x p\right)^n_{i+\frac{1}{2}j}+\mathcal{O}(\Delta x^3)\right). \end{aligned}$$

Consequently, and following the same arguments for the vertical fluxes, we have added in the right-hand side of the pressure equation (2.9) the following small regularizing term:

$$\left(\frac{1}{\Delta t}+\frac{\nu}{\Delta x^2}+\frac{\nu}{\Delta y^2}\right)^{-1}\left(\frac{\Delta x^2}{4}\left(\partial^4_x p\right)^n_{ij}+\frac{\Delta y^2}{4}\left(\partial^4_y p\right)^n_{ij}+\mathcal{O}(\Delta x^4)+\mathcal{O}(\Delta y^4)\right).$$

So, the idea is to prevent checkerboard oscillations by perturbing the continuity equation with the pressure terms, the basic mathematical principle being that an added small regularizing term annihilates the spurious modes. This term does not cancel the consistency of our scheme but it increases its diffusivity.

Remark 2.4. From the point of view of the stability analysis of this colocated space discretization using a projection method as time discretization, see, e.g., [3] for a stability proof with a linear interpolation for the fluxes. We intend, in a future work, to study the stability of this scheme when the intermediate fluxes are computed with the modified interpolation (2.15). Such a modified interpolation introduces new difficulties which deserve to be studied separately.

3 A colocated finite volume scheme with a splitting method for the time discretization

In their article [7], Guermond and Shen introduced a new class of splitting schemes for incompressible flows, called consistent splitting schemes. Like for the projection scheme described in the previous section, these new schemes only require to solve a set of Helmholtz-type equations for the velocity and a Poisson equation for the pressure. Moreover, the preliminary analysis and the numerical experiments conducted by the authors have shown that the consistent splitting schemes are unconditionally stable and yield full second order accuracy for the velocity and the pressure in both the L^2- and H^1-norms (see [7]). For all these reasons, it seems interesting to study if it is possible to combine their scheme with a colocated space discretization.

The scheme used here is the second-order consistent splitting scheme tested in [7].

3.1 Time discretization

First, let us quickly recall how this second-order consistent splitting scheme is built.

We start by choosing a time discretization for (1.1):

$$\frac{3\mathbf{u}^{n+1}-4\mathbf{u}^n+\mathbf{u}^{n-1}}{2\Delta t}-\nu\triangle\mathbf{u}^{n+1}+\hat{\mathcal{B}}\left(\mathbf{u}^n,\mathbf{u}^{n-1}\right)+2\nabla p^n-\nabla p^{n-1}=\mathbf{f}^{n+1}, \tag{3.1}$$

where

$$\hat{\mathcal{B}}\left(\mathbf{u}^n,\mathbf{u}^{n-1}\right)=2\left(\mathbf{u}^n\cdot\nabla\mathbf{u}^n\right)-\left(\mathbf{u}^{n-1}\cdot\nabla\mathbf{u}^{n-1}\right).$$

From this scheme, we are able to compute the new velocity $\mathbf{u}^{n+1}$.

Then, to obtain the pressure, we take the divergence of (1.1) and use the incompressibility condition to find:

$$\triangle p=div(\mathbf{f}+\nu\triangle\mathbf{u}-(\mathbf{u}\cdot\nabla)\mathbf{u}). \tag{3.2}$$

The time discretization for the above equation is:

$$\triangle p^{n+1} = div\Big(\mathbf{f}^{n+1} + \nu\triangle\mathbf{u}^{n+1} - \hat{\mathcal{B}}\big(\mathbf{u}^n,\mathbf{u}^{n-1}\big)\Big). \tag{3.3}$$

Following [7], we replace in (3.3) $\triangle$ by $-\nabla\times\nabla\times$. In this way, the accuracy of the splitting scheme will be improved [7], and we obtain:

$$\triangle p^{n+1} = div\Big(\mathbf{f}^{n+1} - \nu\nabla\times\nabla\times\mathbf{u}^{n+1} - \hat{\mathcal{B}}\big(\mathbf{u}^n,\mathbf{u}^{n-1}\big)\Big). \tag{3.4}$$

Using the well-known relation:

$$\triangle\mathbf{u}^{n+1} = \nabla div\,\mathbf{u}^{n+1} - \nabla\times\nabla\times\mathbf{u}^{n+1}, \tag{3.5}$$

(3.1) becomes:

$$\begin{aligned} &\mathbf{f}^{n+1} - \nu\nabla\times\nabla\times\mathbf{u}^{n+1} - \hat{\mathcal{B}}\big(\mathbf{u}^n,\mathbf{u}^{n-1}\big) \\ =&\frac{3\mathbf{u}^{n+1} - 4\mathbf{u}^n + \mathbf{u}^{n-1}}{2\Delta t} - \nu\nabla div\,\mathbf{u}^{n+1} + 2\nabla p^n - \nabla p^{n-1}. \end{aligned} \tag{3.6}$$

Inserting the previous equation in (3.4), we obtain:

$$\triangle p^{n+1} = div\left(\frac{3\mathbf{u}^{n+1} - 4\mathbf{u}^n + \mathbf{u}^{n-1}}{2\Delta t} - \nu\nabla div\,\mathbf{u}^{n+1} + 2\nabla p^n - \nabla p^{n-1}\right). \tag{3.7}$$

Hence:

$$\triangle\left(p^{n+1} - 2p^n + p^{n-1} + \nu div\,\mathbf{u}^{n+1}\right) = div\left(\frac{3\mathbf{u}^{n+1} - 4\mathbf{u}^n + \mathbf{u}^{n-1}}{2\Delta t}\right). \tag{3.8}$$

In summary, the time discretization obtained by following the method of [7], consists in computing the velocity $\mathbf{u}^{n+1}$ with the equation (3.1) according to the Dirichlet boundary conditions:

$$\begin{cases} \dfrac{3\mathbf{u}^{n+1} - 4\mathbf{u}^n + \mathbf{u}^{n-1}}{2\Delta t} - \nu\triangle\mathbf{u}^{n+1} + \hat{\mathcal{B}}\big(\mathbf{u}^n,\mathbf{u}^{n-1}\big) + 2\nabla p^n - \nabla p^{n-1} = f^{n+1}, \\ \text{where} \quad \hat{\mathcal{B}}\big(\mathbf{u}^n,\mathbf{u}^{n-1}\big) = 2\big(\mathbf{u}^n\cdot\nabla\mathbf{u}^n\big) - \big(\mathbf{u}^{n-1}\cdot\nabla\mathbf{u}^{n-1}\big), \\ \mathbf{u}^{n+1}\Big|_{\partial\Omega} = \mathbf{g}. \end{cases} \tag{3.9}$$

Then we compute the pressure p^{n+1} from:

$$\begin{cases} \triangle\psi^{n+1} = div\left(\dfrac{3\mathbf{u}^{n+1} - 4\mathbf{u}^n + \mathbf{u}^{n-1}}{2\Delta t}\right), \\ \dfrac{\partial\psi^{n+1}}{\partial\mathbf{n}} = 0, \end{cases} \tag{3.10}$$

$$p^{n+1} = \psi^{n+1} + 2p^n - p^{n-1} - \nu div\,\mathbf{u}^{n+1}. \tag{3.11}$$

The main advantage of this splitting scheme is that it is no longer plagued by the artificial Neumann boundary condition of p^{n+1} (see (2.4)).

3.2 Finite volume discretization

To derive the colocated finite volume discretization associated with this time discretization, we integrate the equations (3.9)-(3.11) on each control volume K_{ij}. In doing so, we keep the notations used in the previous section and also the method used to integrate each term. Concerning the boundary conditions, we have a Dirichlet boundary condition for $\mathbf{u}^{n+1}$:

$$\begin{aligned}&\frac{\mathbf{u}^{n+1}_{M+1j}+\mathbf{u}^{n+1}_{Mj}}{2}=\mathbf{g}^{n+1}_{M+\frac{1}{2}j}, \quad &&\frac{\mathbf{u}^{n+1}_{0j}+\mathbf{u}^{n+1}_{1j}}{2}=\mathbf{g}^{n+1}_{\frac{1}{2}j},\\ &\frac{\mathbf{u}^{n+1}_{i0}+\mathbf{u}^{n+1}_{i1}}{2}=\mathbf{g}^{n+1}_{i\frac{1}{2}}, &&\frac{\mathbf{u}^{n+1}_{iN+1}+\mathbf{u}^{n+1}_{iN}}{2}=\mathbf{g}^{n+1}_{iN+\frac{1}{2}},\end{aligned} \tag{3.12}$$

and a Neumann boundary condition for ψ^{n+1}:

$$\psi^{n+1}_{M+1j}=\psi^{n+1}_{Mj}, \quad \psi^{n+1}_{0j}=\psi^{n+1}_{1j}, \quad \psi^{n+1}_{iN+1}=\psi^{n+1}_{iN}, \quad \psi^{n+1}_{i0}=\psi^{n+1}_{i1}. \tag{3.13}$$

Remark 3.1. In (3.9), the terms p_{0j}, p_{M+1j}, p_{i0} and p_{iN+1} occur in the gradient of the pressure, but they are not given by the boundary conditions. Consequently, we use a second order compact scheme [11] to compute them:

$$\begin{aligned}&p_{0j}=\frac{5}{2}p_{1j}-2p_{2j}+\frac{1}{2}p_{3j}, \quad &&p_{M+1j}=\frac{5}{2}p_{Mj}-2p_{M-1j}+\frac{1}{2}p_{M-2j},\\ &p_{i0}=\frac{5}{2}p_{i1}-2p_{i2}+\frac{1}{2}p_{i3}, &&p_{iN+1}=\frac{5}{2}p_{iN}-2p_{iN-1}+\frac{1}{2}p_{iN-2}.\end{aligned} \tag{3.14}$$

Finally, the two steps of the algorithm are the following ones:

1. We compute the new velocities $\mathbf{u}^{n+1}=\left(u^{n+1},v^{n+1}\right)$ from:

$$\begin{aligned}&\Delta x\Delta y\frac{3\mathbf{u}^{n+1}_{ij}-4\mathbf{u}^{n}_{ij}+\mathbf{u}^{n-1}_{ij}}{2\Delta t}-\nu\left[\Delta y\frac{\mathbf{u}^{n+1}_{i+1j}-\mathbf{u}^{n+1}_{ij}}{\Delta x}+\Delta y\frac{\mathbf{u}^{n+1}_{i-1j}-\mathbf{u}^{n+1}_{ij}}{\Delta x}\right.\\ &\left.+\Delta x\frac{\mathbf{u}^{n+1}_{ij+1}-\mathbf{u}^{n+1}_{ij}}{\Delta y}+\Delta x\frac{\mathbf{u}^{n+1}_{ij-1}-\mathbf{u}^{n+1}_{ij}}{\Delta y}\right]+2\begin{pmatrix}\frac{\Delta y}{2}\left(p^{n}_{i+1j}-p^{n}_{i-1j}\right)\\ \frac{\Delta x}{2}\left(p^{n}_{ij+1}-p^{n}_{ij-1}\right)\end{pmatrix}\\ &-\begin{pmatrix}\frac{\Delta y}{2}\left(p^{n-1}_{i+1j}-p^{n-1}_{i-1j}\right)\\ \frac{\Delta x}{2}\left(p^{n-1}_{ij+1}-p^{n-1}_{ij-1}\right)\end{pmatrix}+\hat{\mathcal{B}}\left(\mathbf{u}^{n},\mathbf{u}^{n-1}\right)_{ij}=\Delta x\Delta y\,\mathbf{f}^{n+1}_{ij},\end{aligned} \tag{3.15}$$

where:

$$
\begin{aligned}
\hat{\mathcal{B}}(\mathbf{u}^n,\mathbf{u}^{n-1})_{ij} =& \Delta y\left[2F^n_{u\,i+\frac{1}{2}j}-F^{n-1}_{u\,i+\frac{1}{2}j}\right]\left[2\frac{\mathbf{u}^n_{i+1j}+\mathbf{u}^n_{ij}}{2}-\frac{\mathbf{u}^{n-1}_{i+1j}+\mathbf{u}^{n-1}_{ij}}{2}\right]\\
&-\Delta y\left[2F^n_{u\,i-\frac{1}{2}j}-F^{n-1}_{u\,i-\frac{1}{2}j}\right]\left[2\frac{\mathbf{u}^n_{i-1j}+\mathbf{u}^n_{ij}}{2}-\frac{\mathbf{u}^{n-1}_{i-1j}+\mathbf{u}^{n-1}_{ij}}{2}\right]\\
&+\Delta x\left[2F^n_{v\,ij+\frac{1}{2}}-F^{n-1}_{v\,ij+\frac{1}{2}}\right]\left[2\frac{\mathbf{u}^n_{ij+1}+\mathbf{u}^n_{ij}}{2}-\frac{\mathbf{u}^{n-1}_{ij+1}+\mathbf{u}^{n-1}_{ij}}{2}\right]\\
&-\Delta x\left[2F^n_{v\,ij-\frac{1}{2}}-F^{n-1}_{v\,ij-\frac{1}{2}}\right]\left[2\frac{\mathbf{u}^n_{ij-1}+\mathbf{u}^n_{ij}}{2}-\frac{\mathbf{u}^{n-1}_{ij-1}+\mathbf{u}^{n-1}_{ij}}{2}\right].
\end{aligned}
$$

Near the boundary, we use (3.12) and Remark 3.1.

2. To compute the pressure p^{n+1}, we first compute ψ^{n+1} from:

$$
\begin{aligned}
&\Delta y\frac{\psi^{n+1}_{i+1j}-\psi^{n+1}_{ij}}{\Delta x}+\Delta y\frac{\psi^{n+1}_{i-1j}-\psi^{n+1}_{ij}}{\Delta x}+\Delta x\frac{\psi^{n+1}_{ij+1}-\psi^{n+1}_{ij}}{\Delta y}+\Delta x\frac{\psi^{n+1}_{ij-1}-\psi^{n+1}_{ij}}{\Delta y}\\
&=\frac{1}{2\Delta t}\left[\Delta y\left[\left(3F^{n+1}_{u\,i+\frac{1}{2}j}-4F^n_{u\,i+\frac{1}{2}j}+F^{n-1}_{u\,i+\frac{1}{2}j}\right)-\left(3F^{n+1}_{u\,i-\frac{1}{2}j}-4F^n_{u\,i-\frac{1}{2}j}+F^{n-1}_{u\,i-\frac{1}{2}j}\right)\right]\right.\\
&\quad\left.+\Delta x\left[\left(3F^{n+1}_{v\,ij+\frac{1}{2}}-4F^n_{v\,ij+\frac{1}{2}}+F^{n-1}_{v\,ij+\frac{1}{2}}\right)-\left(3F^{n+1}_{v\,ij-\frac{1}{2}}-4F^n_{v\,ij-\frac{1}{2}}+F^{n-1}_{v\,ij-\frac{1}{2}}\right)\right]\right],
\end{aligned}
\tag{3.16}
$$

using the boundary conditions (3.13).

Then, we easily obtain the pressure:

$$
p^{n+1}_{ij}=\psi^{n+1}_{ij}+2p^n_{ij}-p^{n-1}_{ij}-\frac{\nu}{\Delta x\Delta y}\left[\Delta y\left(F^{n+1}_{u\,i+\frac{1}{2}j}-F^{n+1}_{u\,i-\frac{1}{2}j}\right)+\Delta x\left(F^{n+1}_{v\,ij+\frac{1}{2}}-F^{n+1}_{v\,ij-\frac{1}{2}}\right)\right]. \tag{3.17}
$$

3.3 Computation of the fluxes

As in Section 2, the way used to interpolate the fluxes is essential because it determines the coupling between the velocities and the pressure. The simplest method, a linear interpolation, is also not sufficient to exclude the spurious modes in the case of this splitting method.

To prevent here the checkerboard oscillations we have used a pressure-weighted interpolation [17] as for the projection method. However, a relaxation coefficient $\theta \le 1$ must be added in front of the small regularizing term in the continuity equation (3.16). This means that the fluxes are computed by:

$$F^{n+1}_{u\,i+\frac{1}{2}j}=\frac{u^{n+1}_{i+1j}+u^{n+1}_{ij}}{2}+\theta\frac{\Delta y}{4a}\left(p^n_{i+2j}-2p^n_{i+1j}+p^n_{ij}\right)-\theta\frac{\Delta y}{4a}\left(p^n_{i+1j}-2p^n_{ij}+p^n_{i-1j}\right),$$

$$F^{n+1}_{v\,ij+\frac{1}{2}}=\frac{v^{n+1}_{ij+1}+v^{n+1}_{ij}}{2}+\theta\frac{\Delta x}{4a}\left(p^n_{ij+2}-2p^n_{ij+1}+p^n_{ij}\right)-\theta\frac{\Delta x}{4a}\left(p^n_{ij+1}-2p^n_{ij}+p^n_{ij-1}\right). \tag{3.18}$$

Remarks 2.2 and 2.3 are still valid (modulo the coefficient θ), and thus justify the fact that the spurious modes are annihilated. In Remark 3.2 we explain why a relaxation θ has to be added in front of the small regularizing term.

Remark 3.2. To explain the influence of θ, we study the order of the left hand side of the continuity equation. In the case of the projection method, we have:

$$\Delta y\frac{\delta p^{n+1}_{i+1j}-\delta p^{n+1}_{ij}}{\Delta x}+\Delta y\frac{\delta p^{n+1}_{i-1j}-\delta p^{n+1}_{ij}}{\Delta x}+\Delta x\frac{\delta p^{n+1}_{ij+1}-\delta p^{n+1}_{ij}}{\Delta y}+\Delta x\frac{\delta p^{n+1}_{ij-1}-\delta p^{n+1}_{ij}}{\Delta y}$$
$$\simeq\Delta x\Delta y\left[\triangle\left(\Delta t p_t\right)\right]^{n+1}_{ij},$$

and for the splitting method we find:

$$\Delta y\frac{\psi^{n+1}_{i+1j}-\psi^{n+1}_{ij}}{\Delta x}+\Delta y\frac{\psi^{n+1}_{i-1j}-\psi^{n+1}_{ij}}{\Delta x}+\Delta x\frac{\psi^{n+1}_{ij+1}-\psi^{n+1}_{ij}}{\Delta y}+\Delta x\frac{\psi^{n+1}_{ij-1}-\psi^{n+1}_{ij}}{\Delta y}$$
$$\simeq\Delta x\Delta y\left[\triangle\left(\Delta t^2 p_{tt}+\nu\, div\mathbf{u}\right)\right]^{n+1}_{ij}.$$

We note that the left-hand side of the continuity equation of the splitting method is smaller than that of the projection method but in both cases the regularizing term has the same order. Moreover, we have also noticed that the splitting method does not work when the regularizing term is too large. So, to control the influence of this added term, we use the relaxation coefficient θ. For $\theta=1/4$, we have obtained for several analytic benchmarks the expected accuracy for the pressure (order 2) without spurious modes. Consequently, we have used this value for all the numerical results presented in the next section. However, for other simulations, it is possible to have to change this value.

4 Numerical results

This section presents the numerical results of the two previously considered time discretizations with the same colocated space discretizations. In the following, we call "PMFV" the scheme using the projection method and we call "GSFV" the scheme using the splitting method of [7].

First, to obtain the space and time accuracies of the schemes, we choose the source term corresponding to an exact solution given as an analytical function. Then, we solve the model problem of the driven cavity flow, in which the fluid is enclosed in a unit square box, with an imposed constant velocity in the horizontal direction on the top (driven) boundary, and a no-slip condition on the remaining walls. At the end of the section, we give some concluding remarks.

4.1 Tests of the spatial and time accuracies

4.1.1 Spatial accuracy

Here, to be able to compute the approximation error, the source term **f** is such that the solution of the problem (1.1)-(1.2) is:

$$\begin{aligned} &p(x,y,t)=\cos(\pi x)\sin(\pi y)\sin(t),\\ &\mathbf{u}(x,y,t)=\big(\pi\sin(2\pi y)\sin^2(\pi x)\sin(t),-\pi\sin(2\pi x)\sin^2(\pi y)\sin(t)\big). \end{aligned} \tag{4.1}$$

To obtain the spatial accuracy of the schemes, we fix the time-step $\Delta t=10^{-3}$ and solve the Navier-Stokes equations using the two methods presented in Sections 2 ("PMFV" method) and 3 ("GSFV" method) with different space steps $\Delta x=\Delta y=1/10,1/20,\cdots,1/60$. Moreover, the final time is $T=1$ and the Reynolds number is $Re=100$.

We show in Fig. 2 the error on the velocity measured in the kinetic energy (L^2-) norm and in the enstrophy (H_0^1-) norm for both methods "PMFV" and "GSFV". In Fig. 3, we present the error on the pressure measured in the L^2-norm.

The results show that, as expected, the velocity and the pressure approximations are second-order accurate for all the norms considered and for both time discretizations.

4.1.2 Time accuracy

Now, we study the time accuracy of the schemes using the same analytical solution (4.1). Here, the expected time order accuracy for the velocity and the pressure is Δt^2, so we must choose a very small space-step $\Delta x \ll \Delta t$ such that the approximation error in space does not become more important than the approximation error in time. In fact, for both methods "PMFV" and "GSFV" when they are used to solve the Navier-Stokes equations, we can not take a small space-step Δx without taking also a very small time-step Δt due to the usual stability condition deriving from the explicit time discretization of the nonlinear term of (1.1)-(1.2). However, to still obtain an idea of the time order accuracy of the schemes, we can circumvent this difficulty by solving the Stokes equations. Consequently, we have removed the nonlinear term in the schemes and we solved the Stokes equations with a fixed space-step $\Delta x=\Delta y=1/200$ and different values for the time step $10^{-2}\le\Delta t\le 5.10^{-1}$. The final time is $T=18$ and the Reynolds number is $Re=100$.

We show in Fig. 4 that the velocity of the "PMFV" and "GSFV" methods are both second-order time accurate in the L^2-norm and in the H_0^1-norm. Moreover, in Fig. 5, the results clearly show that the time order of the pressure approximation of "PMFV" is only equal to 1.6, whereas the pressure approximation of "GSFV" is truly second-order. This difference can be attributed to the presence in the "PMFV" method of numerical

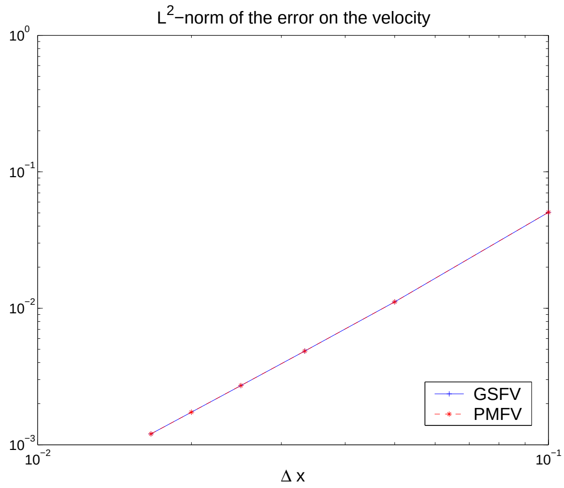

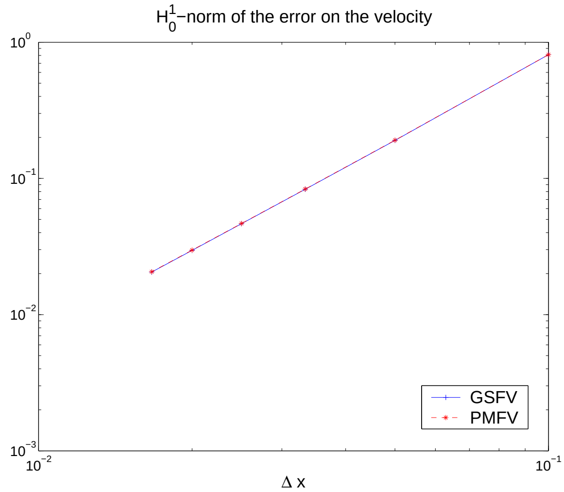

Figure 2: Space discretization error on the velocity at the final time (Navier-Stokes problem, $\Delta t = 10^{-3}$, $Re = 100$).

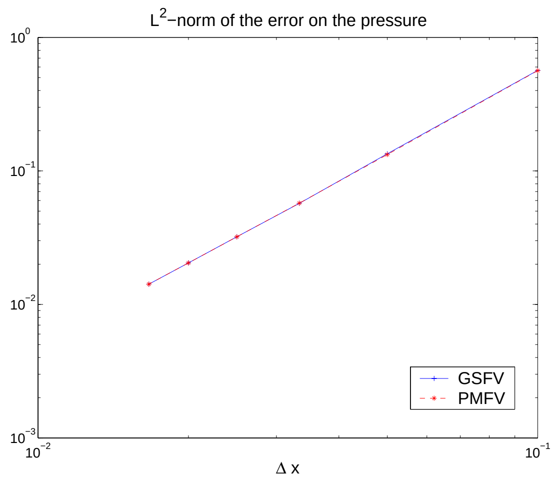

Figure 3: Space discretization error on the pressure at the final time (Navier-Stokes problem, $\Delta t = 10^{-3}$, $Re = 100$).

boundary layers which are induced by the fact that the boundary condition enforced by the approximate pressure, namely $\partial(p^{n+1} - p^n)/\partial \mathbf{n}|_{\partial\Omega}$, is not consistent.

4.2 The driven cavity problem

In a second time, we show the numerical results obtained when we solve the Navier-Stokes problem in the model problem of the driven cavity. The driven boundary conditions are given by:

$$\begin{aligned} \mathbf{g}_{iN+\frac{1}{2}} &= (1,0) \quad \text{for } i = 1,\cdots,M, & \mathbf{g}_{i\frac{1}{2}} &= (0,0) \quad \text{for } i = 1,\cdots,M, \\ \mathbf{g}_{M+\frac{1}{2}j} &= (0,0) \quad \text{for } j = 1,\cdots,N, & \mathbf{g}_{\frac{1}{2}j} &= (0,0) \quad \text{for } j = 1,\cdots,N. \end{aligned}$$

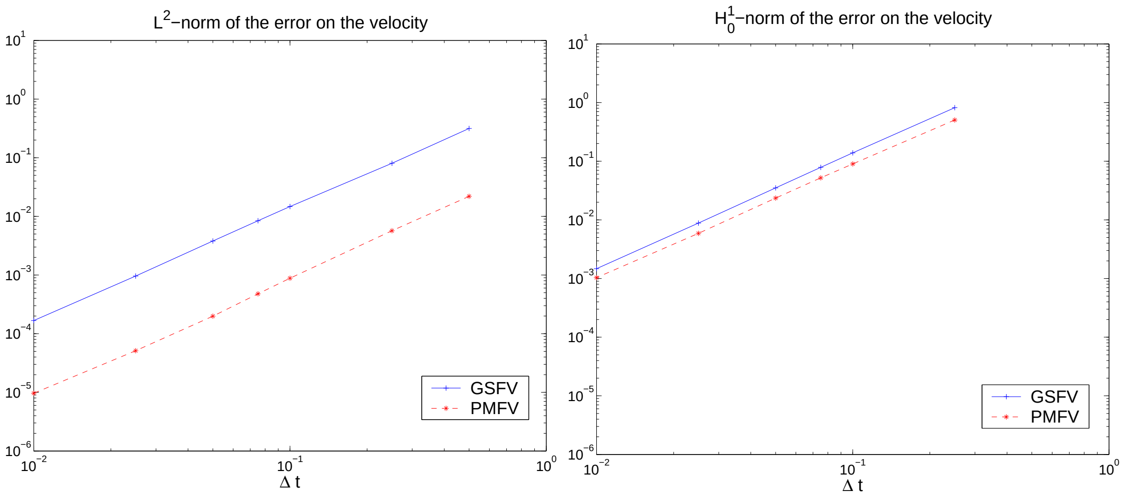

Figure 4: Time discretization error on the velocity at the final time (Stokes problem, $\Delta x = \Delta y = 1/200$, $Re = 100$).

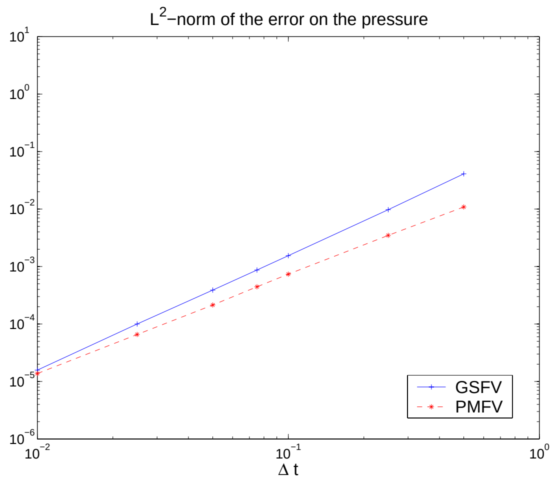

Figure 5: Time discretization error on the pressure at the final time (Stokes problem, $\Delta x = \Delta y = 1/200$, $Re = 100$). The error is of order 2 for GSFV and of order 1.6 only for PMFV.

First, in order to validate the schemes, we compare the velocity profiles of "PMFV" and "GSFV" with the velocity profiles of Ghia [6]. Figs. 6 to 9 show the u-velocity along the vertical line passing through the center and the v-velocity along the horizontal line passing through the center. The computations have been done for several Reynolds numbers, $Re = 100$, 1000, 3200 and 5000, with 128×128 control volumes. The velocity profiles of the schemes "PMFV" and "GSFV" are similar to the results of [6] expect for higher Reynolds numbers, $Re = 3200$ and $Re = 5000$, due to the fact that in [6] a very small space-step is used.

Then, on the next figures, we have drawn the contours of the vorticity, streamfunction and pressure for each scheme for two values of the Reynolds number: $Re = 1000$, Fig. 10 and $Re = 5000$, Fig. 11. Until $Re = 1000$, we do not see any differences on the vorticity,

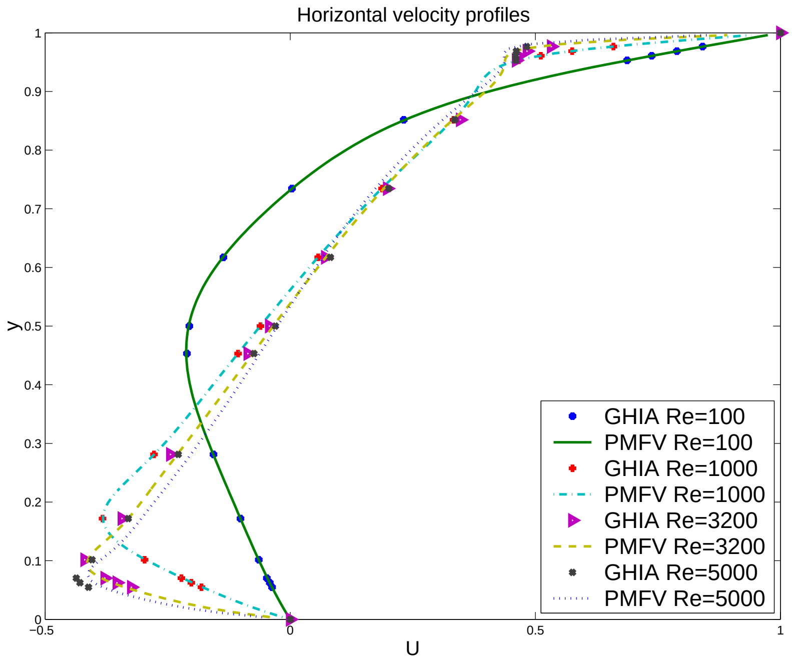

Figure 6: Comparison between "PMFV" and Ghia [6]: the horizontal velocity profiles (Navier-Stokes problem).

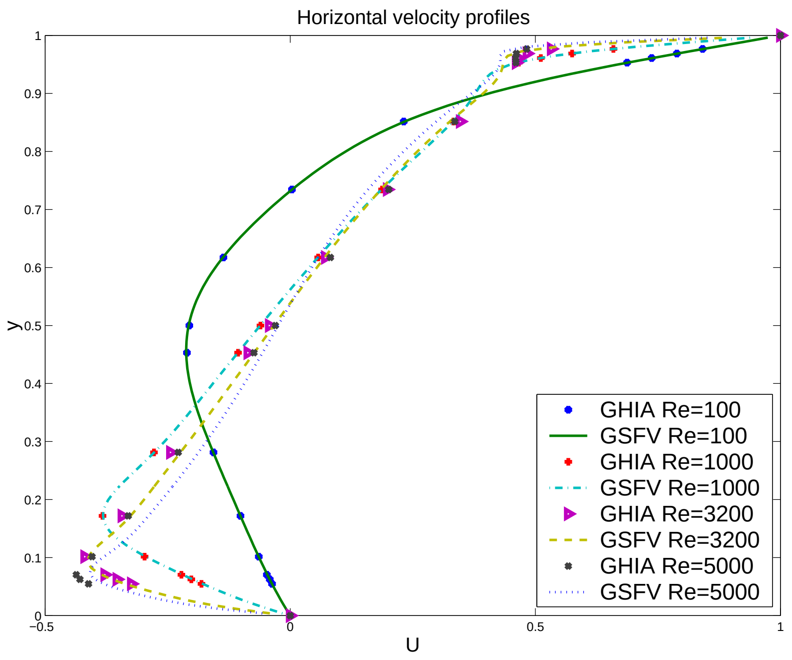

Figure 7: Comparison between "GSFV" and Ghia [6]: the horizontal velocity profiles (Navier-Stokes problem).

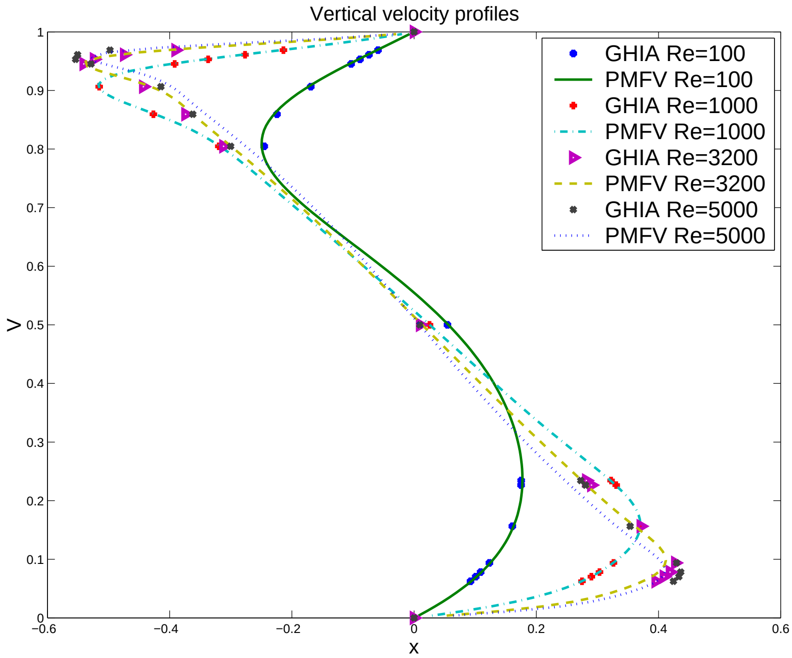

Figure 8: Comparison between "PMFV" and Ghia [6]: the vertical velocity profiles (Navier-Stokes problem).

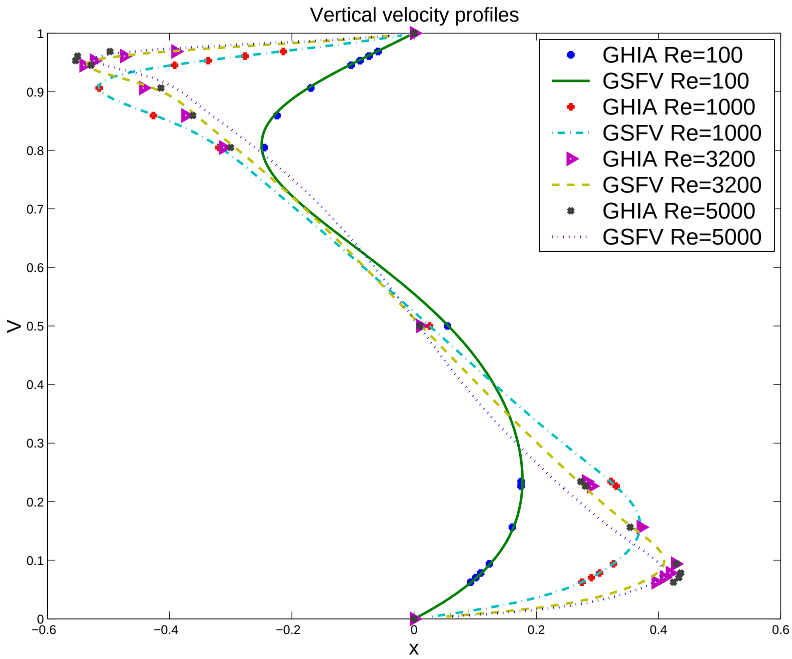

Figure 9: Comparison between "GSFV" and Ghia [6]: the vertical velocity profiles (Navier-Stokes problem).

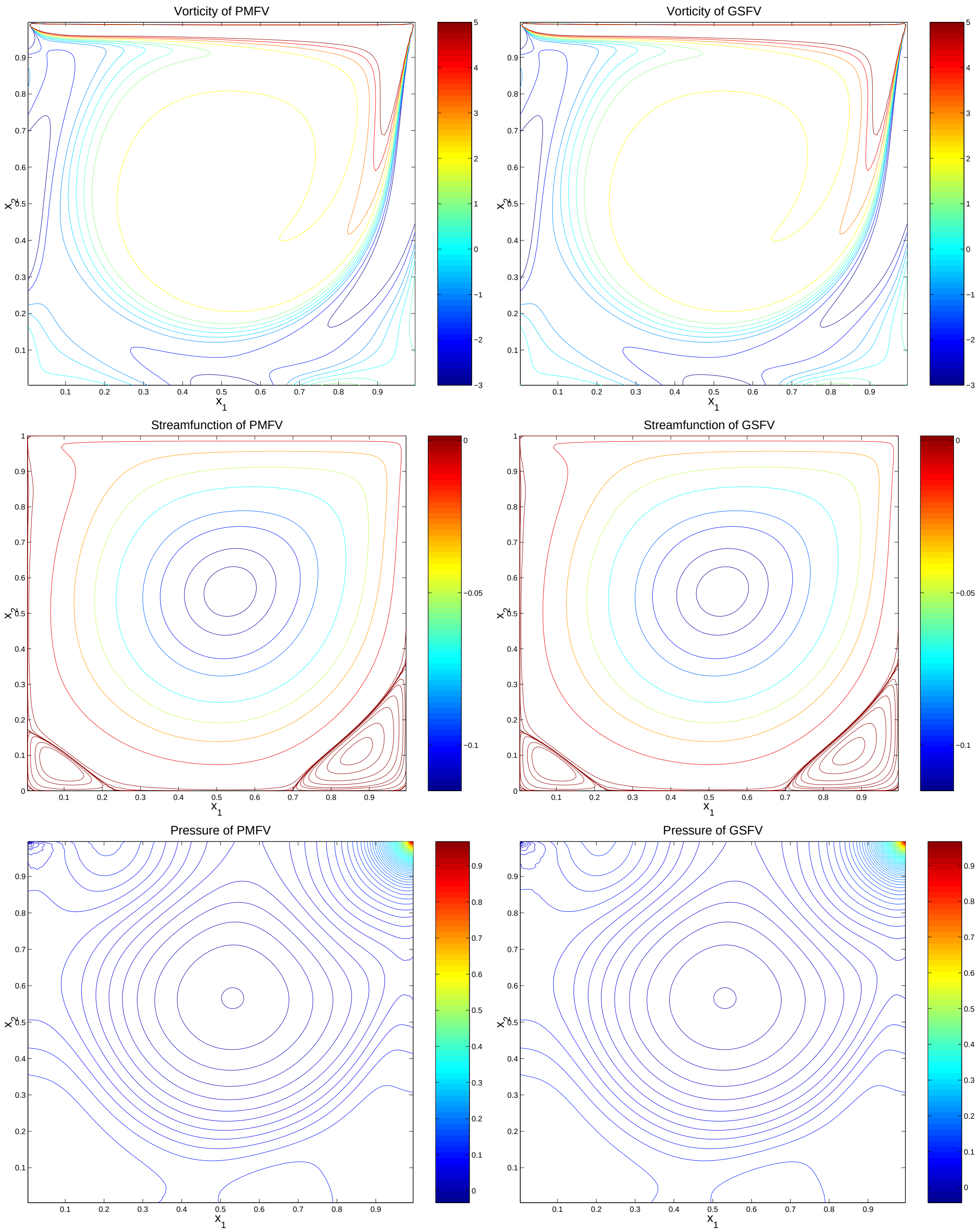

Figure 10: Vorticity, streamfunction and pressure contours for $Re=1000$ (Navier-Stokes problem).

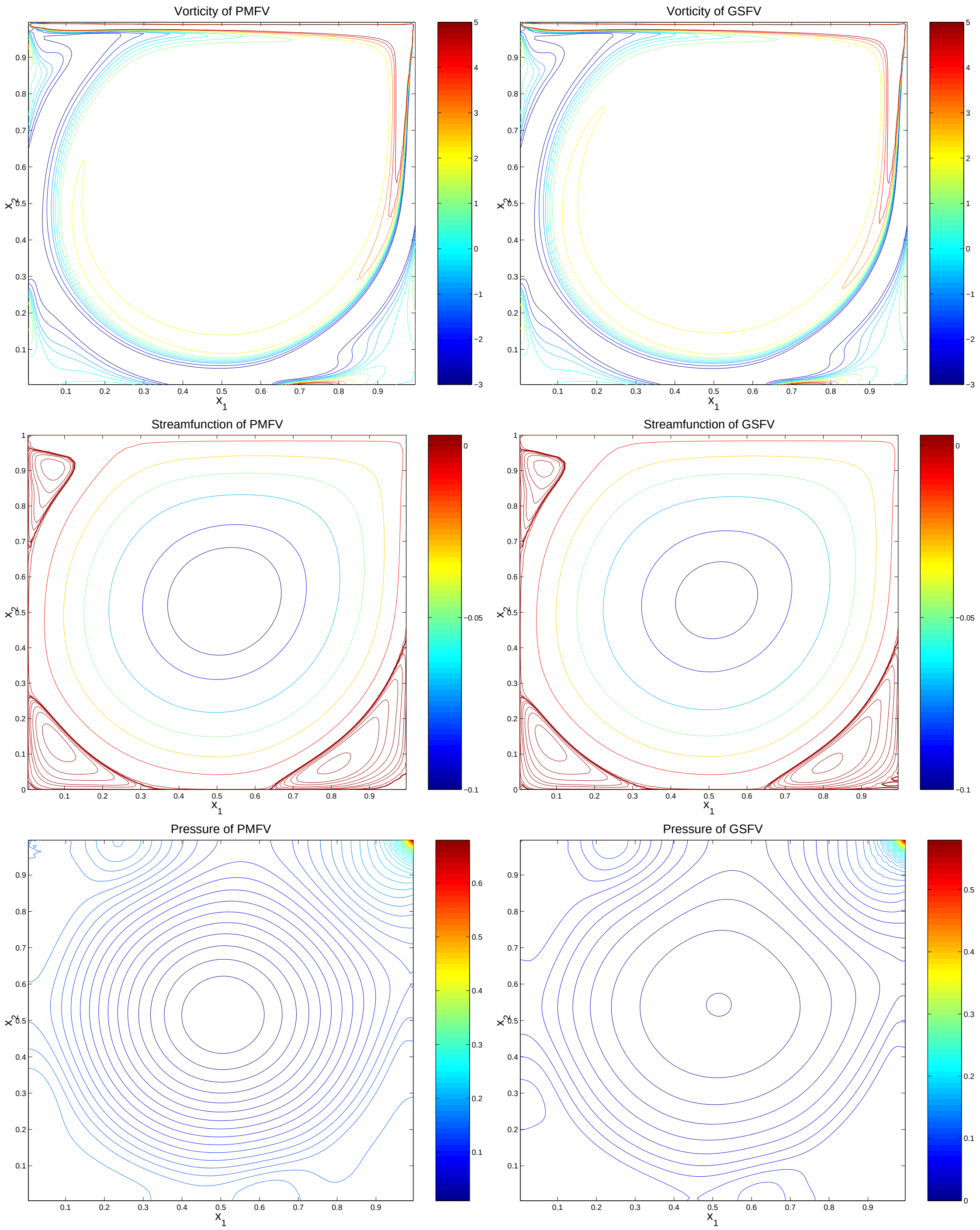

Figure 11: Vorticity, streamfunction and pressure contours for $Re=5000$ (Navier-Stokes problem).

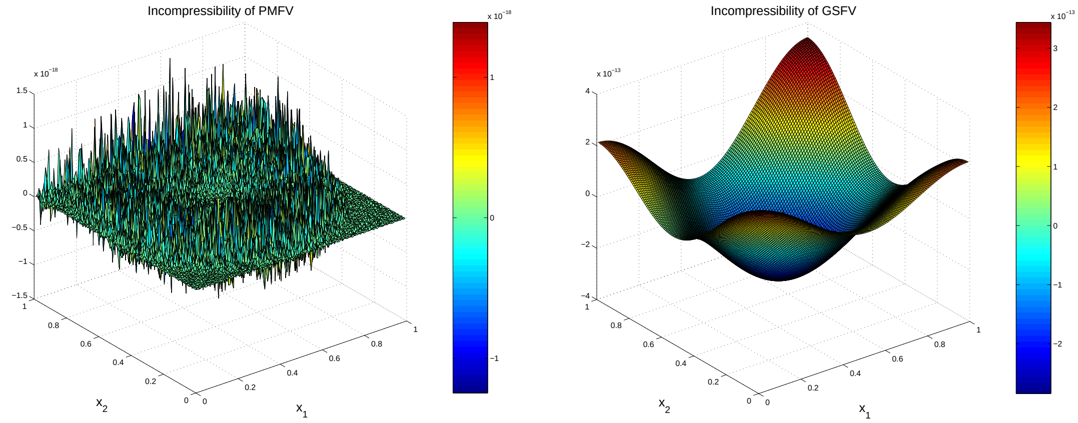

Figure 12: Incompressibilty for $Re=1000$ (Navier-Stokes problem).

streamfunction and pressure contours but when the Reynolds number is higher, some little differences appear on the pressure contours. Moreover, we have also compared the vorticity and streamfunction contours with those of [6] and we have seen that they are similar. Furthermore, note also that we do not have any oscillations on the pressure due to the specific flux interpolations, see Remark 2.3.

Finally, Fig. 12 shows the divergence of the velocities i.e. how the incompressibility condition is satisfied. The divergence is of the order of 10^{-18} for the scheme "PMFV" and of order 10^{-11} for the scheme "GSFV". We are not surprised by this result as it is well-known that for a projection method, the divergence is equal to the computer accuracy, but this is not the case for a splitting method†.

Though the divergence of the velocities is not of the order of the computer accuracy for the scheme "GSFV", since it is smaller than the scheme error (i.e. $\mathcal{O}(\Delta x^2+\Delta y^2)$ and $\mathcal{O}(\Delta t^2)$), it is therefore acceptable.

4.2.1 Concluding remarks

In this paper, we have presented two different time discretizations combined with a finite volume colocated space discretization. We have shown that the colocated space discretization, usually used with a projection method, can also be extended to other time discretizations over previous projection method, like the splitting methods of [7]. The main advantage of this splitting method is that the pressure approximation is truly of second-order.

---

†In the terminology of [7], the projection methods are those introducing an intermediate velocity with an equation like (2.3); the splitting methods do not.

Acknowledgments

The authors thank the reviewers for their careful reading of the manuscript. This work was partially supported by the National Science Foundation under the grant NSF-DMS-0604235, and by the Research Fund of Indiana University.

References

[1] A. J. Chorin, Numerical solution of the Navier-Stokes equations, Math. Comput., 22 (1968), 745-762.

[2] R. Eymard, T. Gallouët, and R. Herbin, Finite volume methods, in: Handbook of Numerical Analysis, Vol. VII, Handb. Numer. Anal., North-Holland, Amsterdam, 2000, pp. 713-1020.

[3] S. Faure, Stability of a colocated finite volume scheme for the Navier-Stokes equations, Numer. Meth. Part. Diff. Equat., 21(2) (2005), 242-271.

[4] S. Faure, J. Laminie and R. Temam, Finite volume discretization and multilevel methods in flow problems, J. Sci. Comput., 25(1-2) (2005), 231-261.

[5] S. Faure, J. Laminie and R. Temam, Finite volume discretization and multilevel methods for the Navier-Stokes equations, In prep., 2008.

[6] U. Ghia, K. N. Ghia and C. T. Shin, High-resolutions for incompressible flow using the Navier-Stokes equations and a multigrid method, J. Comput. Phys., 48 (1982), 387-411.

[7] J. L. Guermond and J. Shen, A new class of truly consistent splitting schemes for incompressible flows, J. Comput. Phys., 192 (2003), 262-276.

[8] J. L. Guermond and J. Shen, Velocity-correction projection methods for incompressible flows, SIAM J. Numer. Anal., 41(1) (2003), 112–134 (electronic).

[9] C. Hsu, A curvilinear-coordinate method for momentum, heat and mass transfer in domains of irregular geometry, PhD thesis, University of Minnesota, 1981.

[10] J. Kim and P. Moin, Application of a fractional-step method to incompressible Navier-Stokes equations, J. Comput. Phys., 59(2) (1985), 308-323.

[11] S. K. Lele, Compact finite difference schemes with spectral-like resolution, J. Comput. Phys., 103(1) (1992), 16-42.

[12] G. I. Marchouk, Numerical Methods in Meteorology, Novosibirsk (in Russian), 1965.

[13] M. Marion and R. Temam, Navier-Stokes equations: Theory and approximation, in: Handbook of Numerical Analysis, Vol. VI, North-Holland, Amsterdam, 1998, pp. 503-688.

[14] S. V. Patankar, Numerical Heat Transfer and Fluid Flow, Series in Computational Methods in Mechanics and Thermal Sciences, McGraw-Hill, New York, 1980.

[15] M. Perić, R. Kessler and G. Sheuerer, Comparison of finite-volume numerical methods with staggered and colocated grids, Comput. Fluids, 16(4) (1988), 389-403.

[16] C. Prakash, A finite element method for predicting flow through ducts with arbitrary cross sections, PhD Thesis, University of Minnesota, 1981.

[17] C. M. Rhie and W. L. Chow, Numerical study of the turbulent flow past an airfoil with trailing edge separation, AIAA J., 21(11) 1983, 1525-1532.

[18] C. M. Rhie, A numerical study of the flow past an isolated airfoil with separation, PhD Thesis, University of Illinois, Urbana-Champaign, 1981.

[19] J. Shen, On error estimates of projection methods for Navier-Stokes equations: Second-order schemes, Mathematica (Cluj), 65(215) (1996), 1039-1065.

[20] R. Temam, Sur l'approximation de la solution des equations de Navier-Stokes par la méthode des pas fractionnaires, I et II, Arch. Rational Mech. Anal., 32(2) (1969), 135-153.

[21] J. Van Kan, A second-order accurate pressure-correction scheme for viscous incompressible flow, SIAM J. Sci. Statist. Comput., 7 (1986), 870-891.

[22] P. Wesseling, Principles of Computational Fluid Dynamics, Springer Series in Computational Mathematics, Vol 29, Springer-Verlag, Germany, 2001.

[23] N. N. Yanenko, The Method of Fractional Steps. The Solution of Problems of Mathematical Physics in Several Variables, Novosibirsk, 1966 (in Russian), English translation, Springer-Verlag, New York, 1971.

[24] N. N. Yanenko and B. G. Kuznetsov, Numerical study of a symmetrical visquous incompressible flow around a disc, in: Symposium of Numerical Calculus and of Applied Mathematics, Novosibirsk, 1965.

[25] Y. Zang, R. L. Street and J. R. Koseff, A non-staggered grid, fractional step method for time-dependent incompressible Navier-Stokes equations in curvilinear coordinates, J. Comput. Phys., 114(1) (1994), 18-33.